



## Research article

## How suspended solids concentration affects nitrification rate in microalgal-bacterial photobioreactors without external aeration



Paola Foladori, Serena Petrini\*, Gianni Andreottola

Department of Civil, Environmental and Mechanical Engineering, University of Trento, via Mesiano 77, 38123, Trento, Italy

## ARTICLE INFO

## Keywords:

Chemical engineering  
 Environmental science  
 Microalgal-bacterial consortia  
 Nitrification  
 Photo-oxygenation  
 Self-shading  
 Biomass concentration  
 Environmental engineering  
 Water treatment  
 Environmental pollution  
 Water pollution  
 Wastewater management

## ABSTRACT

The use of microalgae for the treatment of municipal wastewater makes possible to supply oxygen and save energy, but must be coupled with bacterial nitrification to obtain nitrogen removal efficiency above 90%. This paper explores how the concentration of Total Suspended Solids (TSS, from 0.2 to 3.9 g TSS/L) affects the nitrification kinetic in three microalgal-bacterial consortia treating real municipal wastewater. Two different behaviors were observed: (1) solid-limited kinetic at low TSS concentrations, (2) light-limited kinetic at higher concentrations. For each consortium, an optimal TSS concentration that produced the maximum volumetric ammonium removal rate (around 1.8–2.0 mg N L<sup>-1</sup> h<sup>-1</sup>), was found. The relationship between ammonium removal rate and TSS concentration was then modelled considering bacteria growth, microalgae growth and limitation by dissolved oxygen and light intensity. Assessment of the optimal TSS concentrations makes possible to concentrate the microbial biomass in a photobioreactor while ensuring high kinetics and a low footprint.

## 1. Introduction

Ammonium oxidation is mandatory in sensitive areas due to eutrophication risks and its toxicity for aquatic life (inter alia Kennish and de Jonge, 2011). In municipal wastewater treatment plants (WWTPs) ammonium undergoes full nitrification, a process with a considerable effect on the design, footprint and costs (Jaramillo et al., 2018). In particular, very high electrical energy is required to supply a large amount of external oxygen for nitrification (Åmand et al., 2013; Luo et al., 2019).

Within this context, in recent years, microalgal-bacteria consortia have gained increasing attention as they are able to produce an ideal self-sustaining system that treat wastewater with high ammonium removal efficiency (Subashchandrabose et al., 2011; Liu et al., 2017; Wang et al., 2018). Although both microalgae and cyanobacteria (hereafter referred to as microalgae) are able to utilize various forms of nitrogen, with ammonium being preferred (Krustok et al., 2016; Wang et al., 2016), this direct uptake of nitrogen is not enough to obtain a removal efficiency above 90–95% in municipal wastewater with competitive HRT (Hydraulic retention Time) with respect to activated sludge (Judd et al., 2015). Combination with bacterial nitrification is thus a likely solution (Leong et al., 2018; Vargas et al., 2016; González-Fernández et al., 2011; Rada-Ariza et al., 2017; Ye et al., 2018).

Photosynthetic oxygenation makes it possible to sustain organic matter removal and nitrification without the need for external energy, except natural light. At the same time, CO<sub>2</sub> resulting from organic matter decomposition is fixed by microalgae. In this way, wastewater treatment can be achieved saving energy and mitigating CO<sub>2</sub> (Vu and Loh, 2016; Gonçalves et al., 2017).

While open system as high rate algae ponds (HRAPs) can only be controlled to a limited extent, closed photo-bioreactors (PBRs) are more suitable for optimization and efficient nitrification (Karya et al., 2013; Wang et al., 2018). However, in PBRs, important design parameters such as kinetics have been largely overlooked (Decostere et al., 2016) and the removal process appears slower and less robust than activated sludge (Judd et al., 2015). This may arise mainly from some limitations, such as the lower biomass concentration in PBRs compared to activated sludge and the lower volumetric ammonium removal rates.

In aerated suspended solids processes, as activated sludge, an increase in the concentration of solids is expected to produce higher volumetric removal rates (Henze et al., 2008) and thus a smaller volume and footprint for the plant, if a sufficient amount of external oxygen is provided. However, in microalgal-bacteria based systems an excessive increase in solids concentration may reduce the light penetration, causing self-shading, reducing in-situ photosynthetic oxygenation and limiting

\* Corresponding author.

E-mail address: [serena.petrini@unitn.it](mailto:serena.petrini@unitn.it) (S. Petrini).<https://doi.org/10.1016/j.heliyon.2019.e03088>

Received 24 September 2019; Received in revised form 2 December 2019; Accepted 17 December 2019

2405-8440/© 2019 The Author(s). Published by Elsevier Ltd. This is an open access article under the CC BY-NC-ND license (<http://creativecommons.org/licenses/by-nc-nd/4.0/>).

the overall microbial oxidation kinetic (Anbalagan et al., 2017). Knowledge of the optimal solids concentration in a given microalgal-bacterial system is therefore of extreme importance (Sun et al., 2019).

A very broad range of solids concentrations, from 0.1 to 8 g TSS/L (TSS, Total Suspended Solids) has been reported with open or closed systems (Judd et al., 2015). In general, the literature recommends not maintaining biomass concentrations at excessively high levels in order to avoid self-shading phenomena (Bilad et al., 2014; Udaiyappan et al., 2017; Luo et al., 2017). However, until now, little has been known about the influence of solids concentration on the performances and kinetics of PBRs and no rational approach and systematic study exist to estimate the optimal value.

This paper explores how solids concentrations (in terms of TSS) affect the kinetics of bacterial nitrification in microalgal-bacteria consortia treating real municipal wastewater, without external aeration. In particular, consortia derived from two different PSBRs (Photo-Sequencing-Batch-Reactors) and composed of bacteria, microalgae and inert compounds were considered.

For each consortium, the ammonium removal rate was experimentally determined through AUR (Ammonium Utilisation Rate) tests at different TSS concentrations. Then the optimal solids concentration was estimated by modelling the ammonium removal rate as a function of TSS. Dissolved oxygen and light intensity were taken into account as limiting factors for bacteria and microalgae, respectively. Since there is not a consolidated mathematical expression to describe light limitation (Béchet et al., 2013), the Monod, Steele and Platt-Jassby models were all regarded. It was speculated that the optimal TSS concentration, for a given system, may depend on floc structure and dimension as well as mixing regime and operational factors (such as light distribution and geometry). The assessment of the optimal TSS concentrations enables the microbial biomass in a PBR to be concentrated rationally, keeping the volumetric ammonium removal rate as high as possible.

This paper provides new insights into the design of PBRs in order to ensure high ammonium removal without external aeration, and to lower footprint.

## 2. Materials and methods

### 2.1. Photo-sequencing batch reactors

Two PSBRs, named PSBR1 and PSBR2, were implemented as described in Foladori et al. (2018b) and managed with continuous feeding of wastewater for two years (performances were partially published in Foladori et al., 2018b). The working volume was set at 1.5 L and 2 L for PSBR1 and PSBR2, respectively. Every 48 h, a volume of 0.75 L

and 0.7 L was fed into PSBR1 and PSBR2, respectively, resulting in a Hydraulic Retention Time (HRT) of 4 d and 5.8 d; in agreement with other experiences in literature that indicate a range between 2 and 6 d (Muñoz and Guieysse, 2006). It is worth noting that these systems were not optimized with respect to the HRT and there was scope for a significant footprint reduction.

The two PSBRs differed in the length of photoperiod as indicated in Figure 1: (1) PSBR1 was continuously illuminated and produced “Consortium 1A” and “Consortium 1B”; (2) PSBR2 alternated light phases and dark phases to simulate real conditions and produced “Consortium 2”.

PSBRs were illuminated with artificial lights arranged on one side of the reactors. Light was supplied to PSBR1 by a fluorescent lamp (F30W/33, General Electric, UK) and to PSBR2 by a led lamp (8 led×0.5 W; Orion, Italy), which provided a constant photosynthetically active radiation (PAR) of 45  $\mu\text{mol photon m}^{-2} \text{s}^{-1}$  and 30  $\mu\text{mol photon m}^{-2} \text{s}^{-1}$ , respectively.

Light intensities were measured with a quantum sensor SQ-520 (Apogee Instruments, USA) near the top of the liquid surface inside the reactors. A constant PAR was applied for two reasons: (1) to exclude the daily and seasonal influence of sunlight fluctuations on the microbial activity and the consequent difficulties in the interpretation of parameters (Lee et al., 2015); (2) to avoid the risk of photoinhibition of the nitrifying bacteria and mitigation of this risk by TSS (Vergara et al., 2016). In this way, only the TSS concentration was considered as affecting light penetration and shading.

External addition of supplementary CO<sub>2</sub> was not required in the PSBRs. The CO<sub>2</sub> produced by bacteria was enough to maintain the pH in the optimal range.

### 2.2. Influent real wastewater

The PSBRs were fed with pre-settled wastewater collected from the Trento Nord municipal WWTP (Italy) which receives the sewerage of about 100,000 population equivalent. No filtration of wastewater was performed before feeding. The average composition of the influent pre-settled wastewater is shown in Table 3.

### 2.3. Microalgal-bacterial consortia

The feeding with real wastewater originated spontaneous microalgal-bacterial consortia composed of heterotrophic and ammonium oxidizing bacteria, eukaryotic microalgae and cyanobacteria. The microorganisms embedded in flocs were characterized by high robustness in response to load fluctuations and good settleability. The development, through natural selection, of such a complex community was favored by real wastewater according to Krustok et al. (2015).

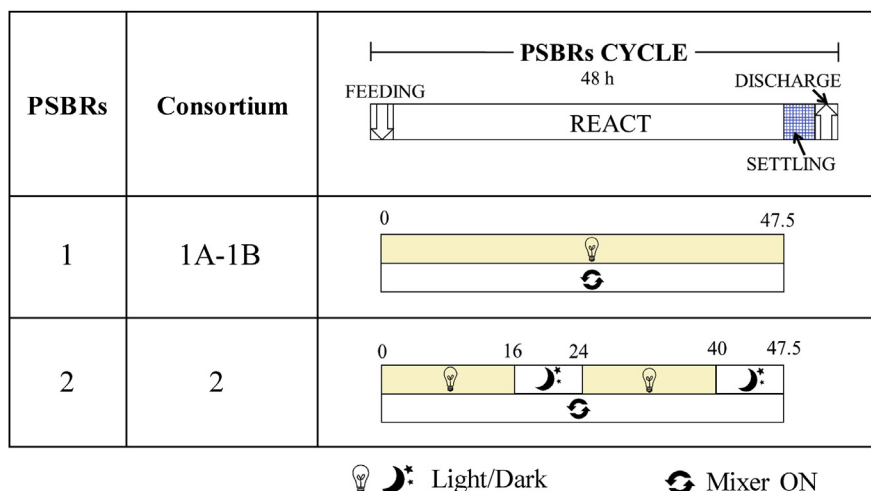


Figure 1. PSBRs cycle and respective consortia. Focus on the applied light and dark conditions.

### 2.4. Analytical methods

Total COD (tCOD; Chemical Oxygen Demand), TSS, TKN (Total Kjeldhal Nitrogen),  $\text{NH}_4^+\text{-N}$ ,  $\text{NO}_2\text{-N}$ ,  $\text{NO}_3\text{-N}$ , Total N and Total P were analyzed according to Standard Methods (APHA, 2002). Soluble COD (sCOD) was measured after filtration of the sample on 0.45- $\mu\text{m}$ -membrane. The parameter TSS in the mixed liquor was measured using the gravimetric method after filtration of the mixed liquor on membranes with a pore size of 0.45  $\mu\text{m}$  and drying at 105 °C. TSS was assumed as a reference for the biomass concentration inside the PSBRs. Although total solids (both suspended or dissolved) may contribute to hindering the passage of light through the solution. TSS analysis was used here instead of total solids as it is the common measurement to quantify solids in WWTPs. To facilitate comparison with conventional activated sludge processes, the most widespread systems worldwide, TSS were therefore considered to be more appropriate here.

Microscopic observations were performed using a Nikon Optiphot EFD-3 Microscope (Nikon, Japan) to morphologically characterize the microalgal-bacterial consortia.

Online probes (all from WTW, Germany) were applied to measure Dissolved Oxygen (DO), temperature and pH continuously in the PSBRs.

### 2.5. AUR tests

Ammonium utilization rate (AUR) was measured for each microalgal-bacterial consortium at various TSS concentrations. The AUR tests were performed in the PSBRs in batch mode.

Prior to start of the AUR test, a sample was analyzed to check ammonium concentration in the PSBR. Then, a known amount of ammonium was added in the PSBR to achieve an initial concentration of approximately 15 mg  $\text{NH}_4^+\text{-N/L}$ . In cases with a pH lower than 7 at the beginning of the test, a buffer solution was added to raise pH to around 8 in order to prevent nitrification inhibition due to low pH. The duration of the test was 4–6 h. Samples were collected every hour and analyzed for  $\text{NH}_4^+\text{-N}$ ,  $\text{NO}_2\text{-N}$  and  $\text{NO}_3\text{-N}$  after filtration on 0.45- $\mu\text{m}$  membranes.

The volumetric AUR was calculated considering the slope of the straight line that interpolates the experimental  $\text{NH}_4^+\text{-N}$  concentrations over time and was expressed as  $\text{mg N L}^{-1} \text{h}^{-1}$ . The specific AUR was calculated dividing the volumetric AUR by the TSS concentration and was expressed as  $\text{mg N g TSS}^{-1} \text{h}^{-1}$ .

AUR tests were performed with the aim of evaluating TSS influence on the nitrification rate. Therefore, each consortium was tested at five different TSS concentrations. Low TSS concentrations were obtained by extracting part of the mixed liquor and diluting the remaining part with effluent wastewater (to not alter the saline composition). High TSS concentrations were obtained reducing the working volume (not exceeding -15%) by extracting the supernatant. To avoid qualitative and quantitative biomass variations, tests were performed within a week with 18 h between consecutive tests.

### 2.6. Modelling the ammonium removal rate

A simple model was implemented to explain the relationship between ammonium removal rate and TSS concentration. In the model, two main processes were considered:

- 1) aerobic growth of nitrifying biomass, responsible for ammonium oxidation and oxygen consumption;
- 2) photoautotrophic growth of microalgae, responsible for the production of oxygen used in nitrification.

#### 2.6.1. Nitrifying bacteria growth

Under constant environmental parameters (temperature and pH) and a non-limiting substrate ( $\text{NH}_4^+$  in this case), the specific growth rate of nitrifying bacteria ( $\mu_N$ ; Eq.1) depends only on their maximum specific

growth rate ( $\mu_{N,\text{max}}$ ) and a limiting factor that is a function of the oxygen concentration ( $S_O$ ) in the mixed liquor.

$$\mu_N = \mu_{N,\text{max}} \cdot f(S_O) \tag{1}$$

#### 2.6.2. Photoautotrophic algal growth

Analogously, in the case of non-limiting factors for microalgae except light, the specific growth rate of microalgae ( $\mu_{\text{ALG}}$ ; Eq. 2) depends on their maximum specific growth rate ( $\mu_{\text{ALG},\text{max}}$ ) and a function of the light intensity (I).

$$\mu_{\text{ALG}} = \mu_{\text{ALG},\text{max}} \cdot f(I) \tag{2}$$

#### 2.6.3. Conceptual model

Using the Activated Sludge Models (ASMs) framework (Henze et al., 2000), a simplified Gujer matrix (Table 1) was written to describe synthetically the processes involved in the production and consumption of the component  $S_O$ . In this matrix,  $\alpha_1$  and  $\alpha_2$  are stoichiometric coefficients, while  $X_N$  and  $X_{\text{ALG}}$  are the concentrations of nitrifying biomass and microalgae biomass, respectively.

From the Gujer matrix, the derivative of  $S_O$  with respect to time was described in Eq. (3).

$$\frac{dS_O}{dt} = -\alpha_1 \cdot \mu_{N,\text{max}} \cdot f(S_O) \cdot X_N + \alpha_2 \cdot \mu_{\text{ALG},\text{max}} \cdot f(I) \cdot X_{\text{ALG}} \tag{3}$$

During the AUR tests, the oxygen produced by microalgae was completely consumed by the nitrifying bacteria, resulting in a constant (zero)  $S_O$ . The derivative  $dS_O/dt$  was therefore zero. Eq. (3) can be rearranged to express  $f(S_O)$  as described in Eq. (4).

$$f(S_O) = \frac{\alpha_2 \cdot \mu_{\text{ALG},\text{max}} \cdot f(I) \cdot X_{\text{ALG}}}{\alpha_1 \cdot \mu_{N,\text{max}} \cdot X_N} \tag{4}$$

The ratio  $X_{\text{ALG}}/X_N$  is a property of a given consortium and does not change during a relatively short AUR test. It can thus be considered as a constant. The terms  $\alpha_1$ ,  $\alpha_2$ ,  $\mu_{N,\text{max}}$  and  $\mu_{\text{ALG},\text{max}}$  are also constant. All these terms were therefore grouped in a single constant value,  $k$ , defined in Eq. (5).

$$k = \frac{\alpha_2 \cdot \mu_{\text{ALG},\text{max}} \cdot X_{\text{ALG}}}{\alpha_1 \cdot \mu_{N,\text{max}} \cdot X_N} \tag{5}$$

In this way, oxygen limitation ( $f(S_O)$ ) was expressed as a simplified function of light limitation ( $f(I)$ ) in Eq. (6).

$$f(S_O) = k \cdot f(I) \tag{6}$$

The specific rate of substrate utilization (in this case ammonium) is related to the specific growth rate of bacteria taking into account the yield coefficient of nitrifiers ( $Y_{X/N}$ ) as described in Eq. (7).

$$\text{Specific ammonium removal rate} = \frac{\mu_N}{Y_{X/N}} = \frac{\mu_{N,\text{max}} \cdot f(S_O)}{Y_{X/N}} \tag{7}$$

Finally, replacing  $f(S_O)$  (Eq. 6) and grouping the constants in the symbol  $k''$ , the specific ammonium removal rate results a function of  $X$  only (see Eq. 8).

**Table 1.** Simplified Gujer matrix considering the two processes affecting the component  $S_O$ .

No.	Process	Component	Process rate
		$S_O$	
1	Aerobic growth of nitrifying bacteria	$-\alpha_1$	$\mu_{N,\text{max}} \cdot f(S_O) \cdot X_N$
2	Photoautotrophic growth of microalgae	$+\alpha_2$	$\mu_{\text{ALG},\text{max}} \cdot f(I) \cdot X_{\text{ALG}}$

$$\text{Specific ammonium removal rate} = k'' \cdot f(I) = \begin{cases} k'' \cdot \frac{I}{K_i + I} = k'' \cdot \frac{I_0 \cdot e^{-k' \cdot X}}{K_i + I_0 \cdot e^{-k' \cdot X}} \text{ (Monod)} \\ k'' \cdot \frac{I}{I_s} \exp\left(1 - \frac{I}{I_s}\right) = k'' \cdot \frac{I_0 \cdot e^{-k' \cdot X}}{I_s} \exp\left(1 - \frac{I_0 \cdot e^{-k' \cdot X}}{I_s}\right) \text{ (Steele)} \\ k'' \cdot \text{Tanh}\left[\frac{\alpha(I - I_c)}{\mu_{\text{ALG,max}}}\right] = k'' \cdot \text{Tanh}\left[\frac{\alpha(I_0 \cdot e^{-k' \cdot X} - I_c)}{\mu_{\text{ALG,max}}}\right] \text{ (Platt - Jassby)} \end{cases} \quad (8)$$

The volumetric ammonium removal rate (Eq. 9) was obtained by multiplying the specific rate (Eq. 8) by the concentration of solids per unit of volume (X).

$$\text{Volumetric ammonium removal rate} = k'' \cdot f(I) \cdot X \quad (9)$$

### 2.6.4. Functions for light limitation

Various functions have been proposed in literature to describe the limitation of light intensity on microalgal growth (Béchet et al., 2013; Wagner et al., 2016). Here three proposals were considered according to Table 2

In the functions of Table 2, the light intensity, I, was expressed according to Lambert-Beer's law (Eq. 10) that considers the attenuation of incident light intensity (I<sub>0</sub>) due to the solid concentration in the reactor (X), while k' is the extinction coefficient.

$$I = I_0 \cdot e^{-k' \cdot X} \quad (10)$$

### 2.7. Statistical analysis

Statistical calculations were done with Microsoft® Excel. To find the best fitting for the experimental results, regression analysis was performed using the least-square method in Microsoft® Excel. This method finds the optimal parameter values by minimizing the sum of the squared residuals (experimental data minus model predictions).

## 3. Results and discussion

### 3.1. Performances of the PSBRs in the removal of TSS, COD and N forms

The PBR configured as a sequencing batch reactor, that includes separated phases for settling and discharge, favored the selection of microalgae–bacteria bioflocs with good settleability in agreement with other studies in the literature (inter alia Arcila and Buitron, 2016).

Mean removal of TSS (Table 3) was 76 ± 18 % in PSBR1 (effluent concentrations of 59 ± 58 mg TSS/L) and 94 ± 8% in PSBR2 (effluent concentrations of 14 ± 18 mg TSS/L), indicating a slightly better performance of PSBR2 in the settling of solids. The microalgal-bacterial consortia developed in the PSBRs were composed of flocs and dense aggregates with a settling velocity comparable to that of efficient

**Table 2.** Functions considered for describing the light limitation, according to Wagner et al. (2016).

Function name	f(I)	Parameters	Reference
Monod	$f(I) = \frac{I}{K_i + I}$	K <sub>i</sub>	Béchet et al. (2013)
Steele	$f(I) = \frac{I}{I_s} \exp\left(1 - \frac{I}{I_s}\right)$	I <sub>s</sub>	Wagner et al. (2016)
Platt-Jassby	$f(I) = \text{tanh}\left[\frac{\alpha(I - I_c)}{\mu_{\text{ALG,max}}}\right]$	I <sub>c</sub> , μ <sub>ALG,max</sub>	Wagner et al. (2016)

granular sludge (data not shown). This aspect is extremely important to sustain cost-efficient microalgae separation by gravity sedimentation, according to other observations in literature (inter alia Tiron et al., 2015).

The removal efficiency of COD (η<sub>COD</sub>) in the PSBRs (Table 3) was calculated according Eq. (11), taking into account the soluble COD in the effluent in order to exclude the influence of non-settleable solids that depends on the structure of the consortia.

$$\eta_{\text{COD}} = \frac{\text{tCOD} - \text{sCOD}}{\text{tCOD}} \cdot 100 \quad (11)$$

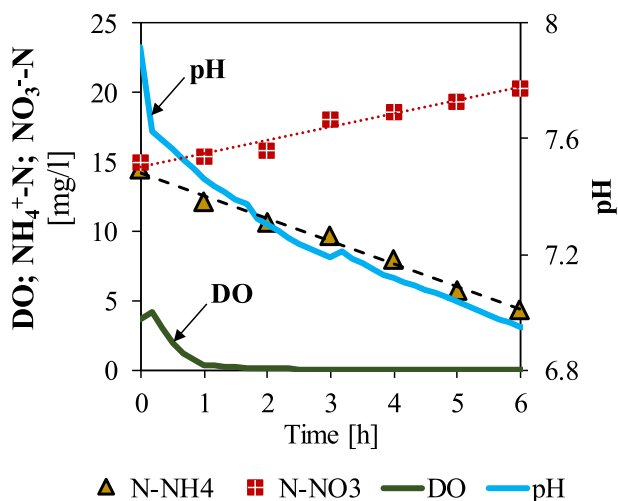
η<sub>COD</sub> was 89 ± 4% and 91 ± 4% in PSBR1 and PSBR2 respectively, with no significant differences among the systems. These values were similar to the efficiency of conventional activated sludge municipal wastewater treatment. It is worth noting that this performance was obtained here without artificial aeration. COD was mainly oxidized by heterotrophic bacteria using DO and nitrates as electron acceptors, although a moderate contribution by microalgae under mixotrophic growth cannot be excluded (Alcantara et al., 2015). The DO for bacteria was produced by photosynthesis, while nitrates were produced from nitrification.

Ammonium removal was 96 ± 7% and 99 ± 2% in PSBR1 and PSBR2, respectively (Table 3), without significant differences between the two systems. This high performance was similar to that of activated sludge, but in the PSBRs the bacterial nitrification was supported by the photosynthetic oxygenation capacity of the microalgal-bacterial consortia. TKN removal was affected by the nitrogen content in the effluent TSS that depends on settling capacity and was thus higher in PSBR2 (Table 3). A significant denitrification was observed especially in PSBR2 under dark conditions, when DO in the PSBR dropped to zero.

Theoretically, total N removal may be attributed to a number of simultaneous processes (Liu et al., 2017): (i) bacterial nitrification followed by denitrification and loss of N<sub>2</sub> in the atmosphere; (ii) biomass uptake of nitrogen, (iii) ammonia stripping and loss in the atmosphere. Here the average Total N removal, 50 ± 14% and 69 ± 10% in PSBR1 and PSBR2 respectively (Table 3), was mainly due to nitrification and partial denitrification. Conversely, N assimilation into biomass was relevant marginally, as a consequence of the small amount of excess sludge produced (data not shown). Ammonia stripping also played a minor role, because pH increased slightly over 9.0 after complete oxidation of the ammonium (Foladori et al., 2018a). Therefore, the low N assimilation and stripping resulted in a considerable availability of NH<sub>4</sub><sup>+</sup> in the mixed liquor, stimulating the development of nitrifying bacteria. Similar observations have been reported by Karya et al. (2013) in a wastewater-treating PBR, where up to 81–85% of ammonium was nitrified by bacteria rather than being taken up by microalgae. Bacterial nitrification in the system is beneficial as it enables two additional benefits to be obtained: (i) avoidance of NH<sub>3</sub> volatilization, which was replaced by the more sustainable emission of denitrified N<sub>2</sub>, (ii) reduction of the inhibitory effects of NH<sub>3</sub> concentration on microalgae growth (Vergara et al., 2016).

**Table 3.** Concentrations of influent and effluent wastewater and removal efficiency in the two PSBRs (mean  $\pm$  standard deviation).

Parameter	Influent concentration (mg/L)	PSBR1		PSBR2	
		Effluent concentration (mg/L)	Removal efficiency (%)	Effluent concentration (mg/L)	Removal efficiency (%)
tCOD	301 $\pm$ 96	99 $\pm$ 6	66 $\pm$ 15	41 $\pm$ 9	85 $\pm$ 6
$\eta_{\text{COD}}$	-	-	89 $\pm$ 4	-	91 $\pm$ 4
TKN	63 $\pm$ 19	7 $\pm$ 4	88 $\pm$ 8	2 $\pm$ 1	97 $\pm$ 2
$\text{NH}_4^+\text{-N}$	54.4 $\pm$ 12.3	1.9 $\pm$ 4.1	96 $\pm$ 7	0.6 $\pm$ 1.1	99 $\pm$ 2
$\text{NO}_2^-\text{-N}$	0.1 $\pm$ 0.1	0.3 $\pm$ 0.7	-	0.1 $\pm$ 0.1	-
$\text{NO}_3^-\text{-N}$	1.1 $\pm$ 0.3	24.4 $\pm$ 8.2	-	18.0 $\pm$ 7.7	-
Total N	63 $\pm$ 18	31 $\pm$ 9	50 $\pm$ 14	20 $\pm$ 8	69 $\pm$ 10
Total P	5.3 $\pm$ 1.7	3.7 $\pm$ 1.9	36 $\pm$ 28	2.6 $\pm$ 0.8	40 $\pm$ 20
TSS	249 $\pm$ 80	59 $\pm$ 58	76 $\pm$ 18	14 $\pm$ 18	94 $\pm$ 8

**Figure 2.** Profiles of  $\text{NH}_4^+\text{-N}$ ,  $\text{NO}_3^-\text{-N}$ , DO and pH during a typical AUR test (example of a test carried out at 1.0 g TSS/L). The slope of the linear fitting of  $\text{NH}_4^+\text{-N}$  data represents the ammonium removal rate.

### 3.2. Measurement of the ammonium removal rates

Figure 2 shows a typical AUR test carried out at a solid concentration of 1.0 g TSS/L. Ammonium concentration and pH decrease while nitrates increase due to bacterial nitrification (Dutta and Sarkar, 2015). During the test, nitrite concentrations may increase up to a few milligrams per liter, but they were depleted after the complete removal of ammonium (data not shown). To calculate the ammonium removal rate, the  $\text{NH}_4^+\text{-N}$  data were interpolated linearly. The  $\text{NH}_4^+\text{-N}$  decrease was considered instead of the  $\text{NO}_3^-\text{-N}$  increase, as nitrate concentration may be underestimated due to the occurrence of simultaneous denitrification in the inner anoxic zone of the flocs.

In the AUR test in Figure 2, the volumetric ammonium removal rate was  $1.6 \text{ mg NH}_4^+\text{-N L}^{-1} \text{ h}^{-1}$ . For a comparison, the transformation rate of  $\text{NH}_4^+\text{-N}$  into  $\text{NO}_3^-\text{-N}$  was evaluated by Tiron et al. (2015) who found values in the range of  $0.14\text{--}1.5 \text{ mg NH}_4^+\text{-N L}^{-1} \text{ h}^{-1}$ . This wide range depended on the level of DO, which varied in that research from zero just after feeding to very high non-limiting values.

With regard to the DO profile during the test in Figure 2, in the presence of  $\text{NH}_4^+$  a long phase with DO constantly near zero was observed (called “zero-DO phase” according to Foladori et al., 2018a). This indicates that the oxygen provided through photosynthesis was used completely for the bacterial nitrification. Despite this zero-DO phase, the process was still proceeding and no significant variations in ammonium removal rate were observed during the test.

### 3.3. Influence of TSS on the ammonium removal rate

A series of AUR tests were performed to measure the ammonium removal rate at different TSS concentrations, from 0.2 to 3.9 g TSS/L considering all the microalgal-bacterial consortia (but under the same PAR and mixing), according to the synthesis in Figure 3. The range of TSS concentrations tested here was wider than others in literature. Garcia et al. (2017) applied biomass concentrations from  $1.2 \pm 0.3 \text{ g TSS/L}$  to  $2.8 \pm 0.3 \text{ g TSS/L}$ . Other studies investigated nutrient removal at concentrations up to  $1.37 \text{ g TSS/L}$  (Judd et al., 2015). Especially when pure algal strains were considered, solid concentrations were relatively low; for example, the maximum concentration was  $1.2 \text{ g/L}$  for *Chlorella* sp. (Li et al., 2011). In this way, the present research contributes by adding results at relatively high TSS concentrations.

The results obtained here are shown in Figure 3, where the volumetric ammonium removal rate (expressed as  $\text{mg N L}^{-1} \text{ h}^{-1}$ ) and the specific ammonium removal rate (expressed as  $\text{mg N g TSS}^{-1} \text{ h}^{-1}$ ) are plotted as a function of the TSS concentration.

#### 3.3.1. The maximum volumetric ammonium removal rate identifies the optimal TSS concentration

For all the consortia, a rise in the volumetric ammonium removal rate occurred when the TSS concentration increased (Figure 3). An optimal condition then appeared, when the nitrification rate reached the maximum value. A further increase in TSS concentration did not provide an advantage in terms of nitrification rate, despite a larger availability of biomass. In fact, for higher solid concentrations, a decrease in the volumetric ammonium removal rate was observed.

In more detail, two parts can be distinguished:

- 1) a first rising part: a higher concentration of solids produces a higher volumetric ammonium removal rate. In this part, the process occurs with enough light and DO, and the nitrification rate is only limited by the amount of biomass (solid-limited kinetic);
- 2) a second decreasing part: a mutual shading of biomass occurs. Light penetration is reduced and nitrification rate is limited by the lower oxygen production rate caused by the increased shadow effect (Udaiyappan et al., 2017) (light-limited kinetic).

Between these parts, the maximum ammonium removal rate identifies the optimal TSS concentration for a system. Different values were observed for each consortium: the optimum was 0.7, 2.6 and  $1.6 \text{ g TSS/L}$  for consortia 1A, 1B and 2, respectively (Figure 3). This difference was associated with the different structure of the flocs, compared in Figure 4, that directly affects the self-shading. In the case of consortia 1A and 2 (Figure 4) the biomass was organized in a larger amount of medium-sized flocs (average floc size of 0.4 mm and 0.2 mm, respectively, Table 4) that formed a higher turbid suspension where self-shading was predominant. Conversely, the structure of consortium 1B (Figure 4) was based on sparse very large granules with an average floc size 0.6 mm (Table 4)

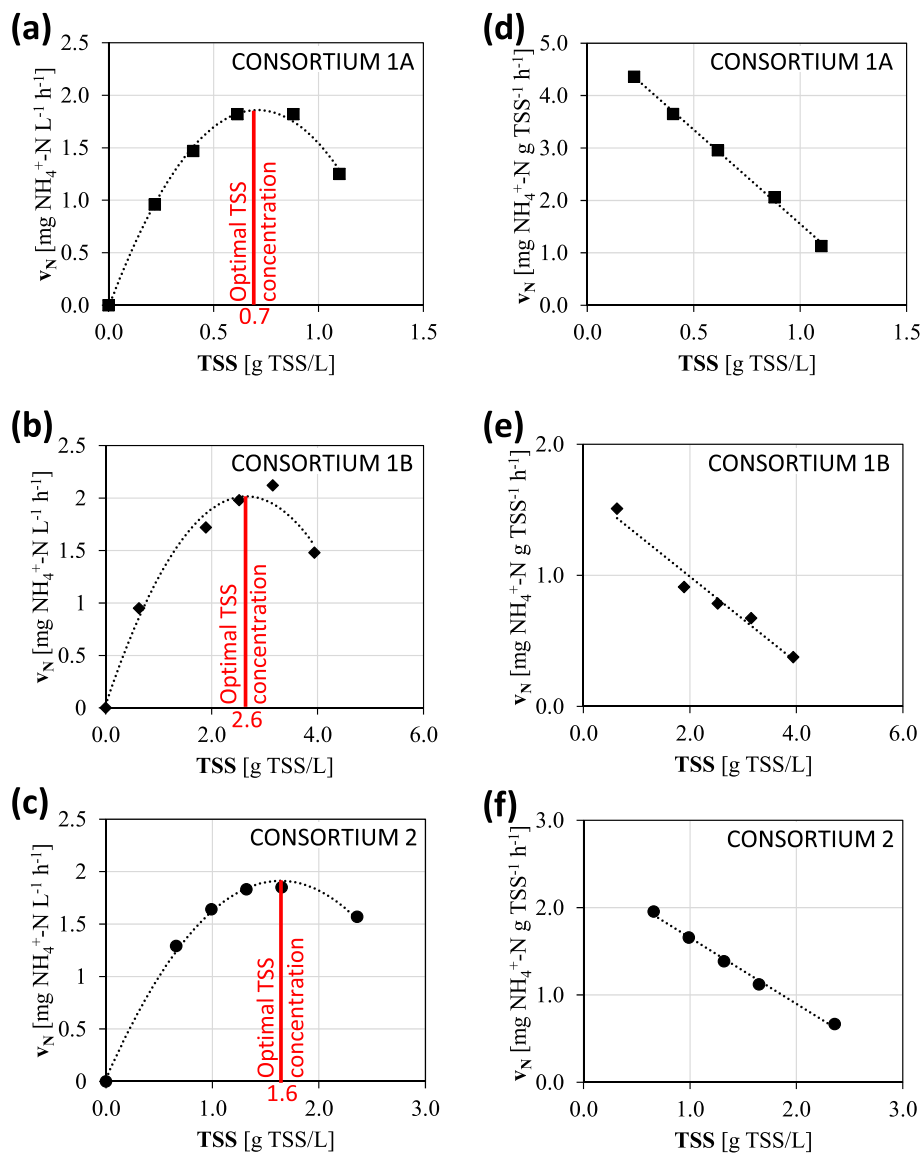


**Figure 3.** Volumetric and specific ammonium removal rate as a function of the TSS concentration for three microalgal-bacterial consortia. (a),(b),(c) Volumetric rate for consortia 1A, 1B and 2, respectively. The optimal TSS concentration that produces the maximum removal rate is indicated for each consortium.(d), (e), (f) Specific rate for consortia 1A, 1B and 2, respectively.

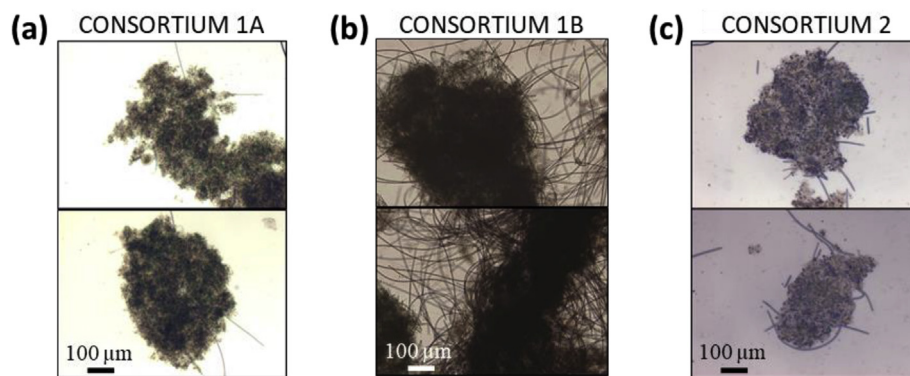


**Figure 4.** Comparison of the flocs structure for the three microalgal-bacterial consortia. (a) consortium 1A, (b) consortium 1B and (c) consortium 2.

**Table 4.** Comparison of the floc size, the TSS concentration and the maximum volumetric ammonium removal rate for the three microalgal-bacterial consortia.

Consortium	Average floc size ( $\mu\text{m}$ )	TSS (g TSS/L)	Maximum volumetric ammonium removal rate ( $\text{mg NH}_4^+\text{-N L}^{-1} \text{h}^{-1}$ )
1A	400	0.7	1.86
1B	600	2.6	2.01
2	200	1.6	1.91

(and up to 1.5 mm) which allowed light to pass more efficiently through the suspension.

### 3.3.2. The volumetric ammonium removal rate is similar among consortia

The maximum volumetric ammonium removal rates (found in correspondence with the optimal TSS concentration) for each microalgal-bacterial consortium are compared in Table 4. The rates were comprised in a small range of 1.8–2.0  $\text{mg NH}_4^+\text{-N L}^{-1} \text{h}^{-1}$ . These values were remarkably higher than other results in literature. The  $\text{NH}_4^+\text{-N}$  transformation rate was up to 1.6  $\text{mg NH}_4^+\text{-N L}^{-1} \text{h}^{-1}$ , as referred by Tiron et al. (2015). Ammonium reduction of 0.81–7.66  $\text{mg NH}_4^+\text{-N L}^{-1} \text{d}^{-1}$  (corresponding to hourly values of up to 0.32  $\text{mg NH}_4^+\text{-N L}^{-1} \text{h}^{-1}$ ) was reported by Rianjo et al. (2012).

The fact that the consortia investigated were characterized by similar maximum ammonium removal rates (Table 4) can be explained by similar TKN loads applied in the PSBRs, that supported a similar growth of nitrifying biomass in the three consortia (nitrification was demonstrated to be the only important process in nitrogen oxidation, see Section 3.1). In other words, the amount of nitrifying bacteria ( $X_N$ , expressed as g VSS/d; VSS = Volatile Suspended Solids) depended on the composition of the influent wastewater and the removed load ( $\Delta\text{TKN}$ , expressed in g TKN/d), according to the relationship in Eq. (12) (Tchobanoglous et al., 2003).

$$X_N = Y_N \cdot \Delta\text{TKN} \quad (12)$$

where  $Y_N$  is the specific yield for nitrifiers (expressed as g VSS<sub>produced</sub>/g TKN<sub>removed</sub>).

Conversely, the amount of microalgal biomass produced in the consortia also depended on the availability of external factors such as light or  $\text{CO}_2$ .

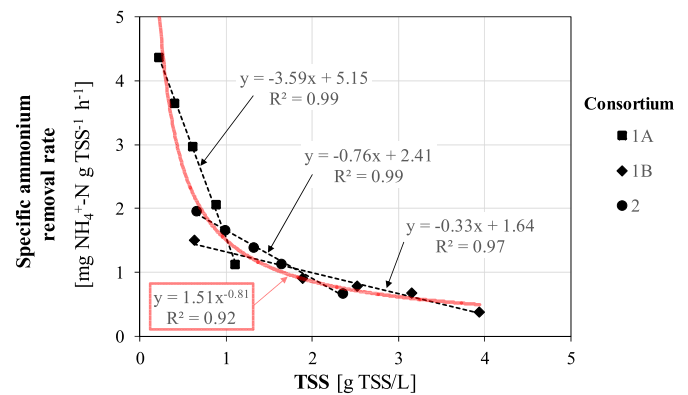
At a given TKN influent load, a consortium developed with a higher TSS concentration does not contain a larger nitrifying biomass, but rather a larger microalgal biomass.

Microscopic observations of the consortia revealed bacteria, microalgae and cyanobacteria embedded with inert solids forming dark green or brown dense flocs and granules (Figure 4). In particular: (1) the consortia 1A and 2 were characterized by the smallest flocs (average floc size of 0.4 mm and 0.2 mm, respectively, Table 4) with a limited presence of filamentous microorganisms; (2) consortium 1B was formed by larger granules with an average floc size of 0.6 mm (Table 4) and it was the consortium with the largest presence of filamentous cyanobacteria. Notwithstanding that consortium 1B, characterized by the highest TSS concentration (i.e. 2.6 g TSS/L), was the richest in photosynthetic cyanobacteria, the nitrification rate was approximately the same (Table 4).

In synthesis, while the amount of nitrifying bacteria in a given consortium is strictly associated with the TKN load in the influent, the microalgal biomass may exploit external resources and may increase freely in the system. Therefore, despite a higher TSS concentration in a consortium, the maximum volumetric nitrification rate is primarily the result of the applied TKN load.

### 3.3.3. The specific ammonium removal rate decreases with TSS concentration

The specific ammonium removal rate as a function of TSS was interpolated with a linear fitting for each consortium (Figure 3). In all

**Figure 5.** Specific ammonium removal rate as a function of TSS for the three microalgal-bacterial consortia.

three cases, the very high regression coefficient ( $R^2 > 97\%$ ) indicated the high strength of the linear correlation.

The comparison between the three consortia is shown in Figure 5, where a clear decreasing behavior can be observed. The higher specific rate of 4.4  $\text{mg NH}_4^+\text{-N g TSS}^{-1} \text{h}^{-1}$  was found at the lowest concentration of 0.2 g TSS/L, while it decreased progressively to 0.4  $\text{mg NH}_4^+\text{-N g TSS}^{-1} \text{h}^{-1}$  (reduction by 91%) at the highest concentration of 3.9 g TSS/L.

A distinct change in slope was observed at a TSS concentration of around 0.6 g TSS/L.

At concentrations  $< 0.6$  g TSS/L (Figure 5), the higher specific removal rates were due to two different but coexisting effects:

- 1) High oxygen production: the scarce biomass permitted an easier passage of light in the reactor and thus the production of oxygen was greater. A higher DO concentration originated an enhanced diffusion of oxygen and thus a larger part of the flocs became aerobic. As a consequence, more biomass was reached by oxygen and the specific ammonium removal rate resulted higher;
- 2) Low oxygen consumption: DO consumption was lower because less bacteria consumed less oxygen. As a consequence a greater availability of oxygen remained for the biomass and the specific rate of nitrifiers resulted higher.

At concentrations  $> 0.6$  g TSS/L (Figure 5), most of the light was absorbed by a thin layer of biomass that produces oxygen only in the external part of the flocs, while lack of light and oxygen occurred in the deeper layers. Other authors have indicated that light shading may occur in PBRs when operating at a biomass concentration higher than 1 g/L (Luo et al., 2017).

Despite the fact that the specific removal rate was higher at low TSS concentrations, it led to an even smaller volumetric rate (expressed as  $\text{mg N L}^{-1} \text{h}^{-1}$ ) due to the low availability of biomass in the PSBR.

In PBRs aimed at obtaining complete wastewater treatment, it is preferable to obtain the highest volumetric ammonium removal rate rather than the highest specific rate, in order to reduce the footprint of the plant. With higher TSS, photosynthesis may be less efficient, but it may be enough to produce a sufficient amount of oxygen to support full nitrification.

### 3.4. Experimental results fit to the simplified model

The experimental results of the specific and volumetric ammonium removal rate were then fitted according to the conceptual model described in Section 2.6.3 and including three different equations to describe light limitation (Table 2). The results are summarized in Figure 6.

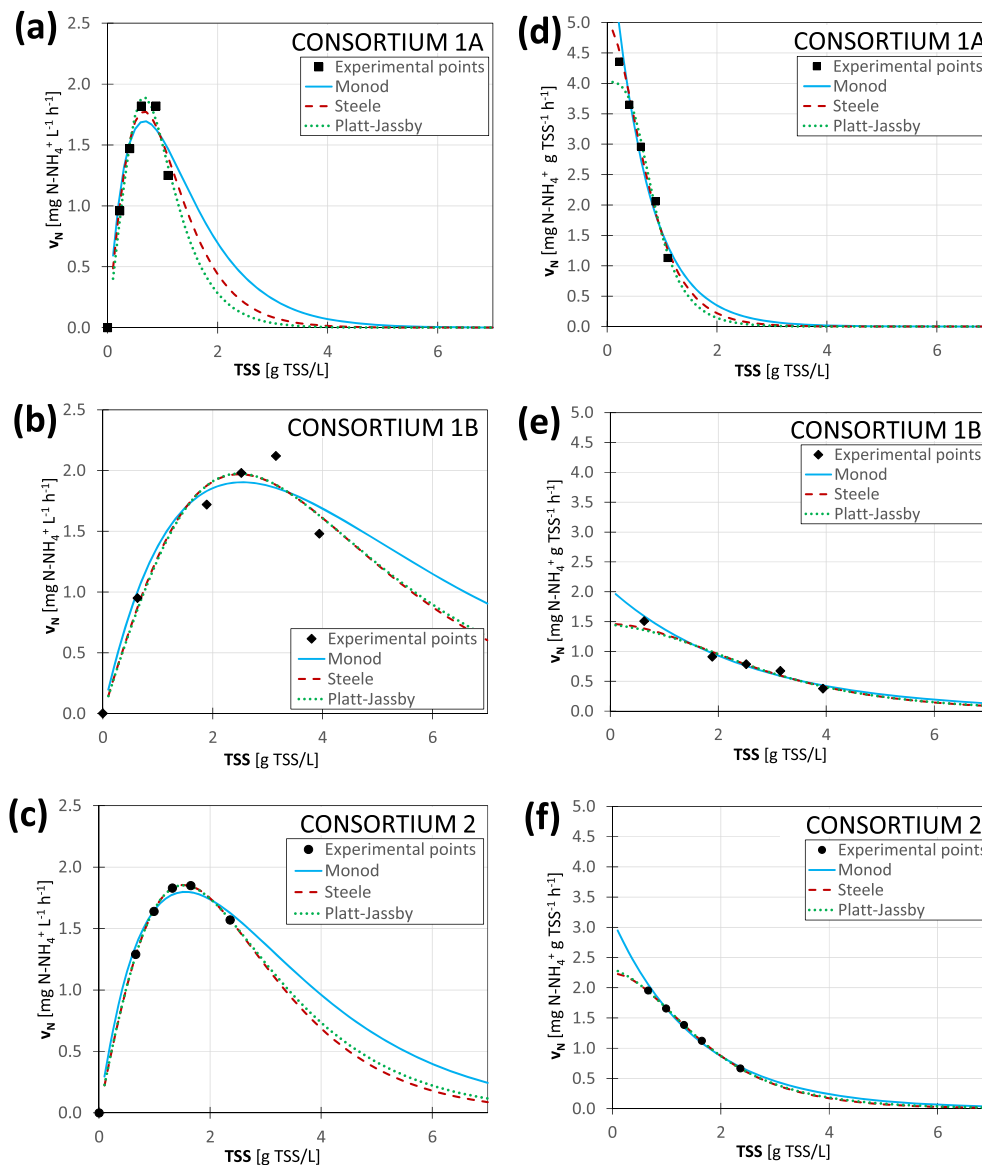


**Figure 6.** Results of the fitting of volumetric and specific ammonium removal rate as a function of the TSS concentration for the three microalgal-bacterial consortia. (a), (b), (c) Volumetric rate for consortia 1A, 1B and 2, respectively. (d), (e), (f) Specific rate for consortia 1A, 1B and 2, respectively.

For all the functions, the model enabled a good fitting of the experimental data to be obtained for both volumetric and specific rates. Monod's equation was slightly worse and this was not surprising as it was based on the simplest form. However, all the fitted curves very clearly confirmed the occurrence of two well defined parts, already observed in section 3.3.1: (1) the rising part, where low TSS and a solid-limited kinetic occurs, (2) the decreasing part where high TSS and a light-limited kinetic occurs and the ammonium removal rate tends progressively to zero.

The model used here for the fitting of the experimental results was able to describe the relationship between the ammonium removal rate and the TSS concentration in a PBR. This finding may help in the management of the complex microalgal-bacterial consortia involved in PBR and to identify the optimal conditions for design.

#### 4. Conclusions

This paper proposes a standardized procedure for measuring both volumetric and specific ammonium removal rate in batch tests under a

given value of irradiance and for a given TSS concentration. Performing 4–5 batch tests at different TSS concentrations with a duration of 4–5 h each, it was possible to identify easily the optimal interval of TSS associated with the maximum ammonium removal rate of the system. When TSS concentration differs from this optimum value, the nitrification kinetic decreases due to: (1) a solid-limited kinetic when TSS is below the optimum, originated by an insufficient amount of biomass in the system, (2) a light-limited kinetic when TSS is above the optimum, due to a less efficient exploitation of light and production of oxygen. The optimal TSS concentration able to produce the maximum volumetric ammonium removal rate (around 1.8–2.0 mg N L<sup>-1</sup> h<sup>-1</sup>) was found for three microalgal-bacterial consortia. A good fitting with a mathematical model (based on bacteria and microalgae growth and limitation by DO and light intensity according to Monod, Steele and Platt-Jassby equations) confirmed the experimental relationship between ammonium removal rate and TSS concentration.

Assessment of optimal solids concentration can thus help in the design of PBRs when enhanced nitrification is required to meet stringent nitrogen limits for the discharge of wastewater.



## Declarations

### Author contribution statement

Paola Foladori: Conceived and designed the experiments; Analyzed and interpreted the data; Wrote the paper.

Serena Petrini: Conceived and designed the experiments; Performed the experiments; Analyzed and interpreted the data; Wrote the paper.

Gianni Andreottola: Critically reviewed the paper.

### Funding statement

This research did not receive any specific grant from funding agencies in the public, commercial, or not-for-profit sectors.

### Competing interest statement

The authors declare no conflict of interest.

### Additional information

No additional information is available for this paper.

### Acknowledgements

The authors would like to thank Andrea Pacini and Mirco Nessenzia for their help during the experimental work.

### References

- Alcantara, C., Posadas, E., Guieysse, B., Munoz, R., 2015. Microalgae-based wastewater treatment. In: Kim, S.K. (Ed.), *Handbook of marine Microalgae*. Biotechnology Advances. Academic Press, London, pp. 439–455.
- Amand, L., Olsson, G., Carlsson, B., 2013. Aeration control – a review. *Water Sci. Technol.* 67, 2374–2398.
- Anbalagan, A., Schwede, S., Lindberg, C., Nehrenheim, E., 2017. Influence of iron precipitated condition and light intensity on microalgae activated sludge based wastewater remediation. *Chemosphere* 168, 1523–1530.
- APHA, AWWA, WEF, 2002. *Standard Methods for the Examination of Water and Wastewater*, 22 ed. American Public Health Association, Washington, D.C.
- Arcila, J.S., Buitrón, G., 2016. Microalgae–bacteria aggregates: effect of the hydraulic retention time on the municipal wastewater treatment, biomass settleability and methane potential. *J. Chem. Technol. Biotechnol.* 91, 2862–2870.
- Béchet, Q., Shilton, A., Guieysse, B., 2013. Modeling the effects of light and temperature on algae growth: state of the art and critical assessment for productivity prediction during outdoor cultivation. *Biotechnol. Adv.* 31, 1648–1663.
- Bilal, M.R., Arafat, H.A., Vankelecom, I.F.J., 2014. Membrane technology in microalgae cultivation and harvesting: A review. *Biotechnol. Adv.* 32, 1283–1300.
- Decostere, B., De Craene, J., Van Hoey, S., Vervaeren, H., Nopens, I., Van Hulle, S., 2016. Validation of a microalgal growth model accounting with inorganic carbon and nutrient kinetics for wastewater treatment. *Chem. Eng. J.* 285, 189–197.
- Dutta, A., Sarkar, S., 2015. Sequencing batch reactor for wastewater treatment: recent advances. *Current Pollution Reports* 1, 177–190.
- Foladori, P., Petrini, S., Andreottola, G., 2018a. Evolution of real municipal wastewater treatment in photobioreactors and microalgae–bacteria consortia using real-time parameters. *Chem. Eng. J.* 345, 507–516.
- Foladori, P., Petrini, S., Nessenzia, M., Andreottola, G., 2018b. Enhanced nitrogen removal and energy saving in a microalgal–bacterial consortium treating real municipal wastewater. *Water Sci. Technol.* 78, 174–182.
- García, D., Alcántara, C., Blanco, S., Pérez, R., Bolado, S., Muñoz, R., 2017. Enhanced carbon, nitrogen and phosphorus removal from domestic wastewater in a novel anoxic–aerobic photobioreactor coupled with biogas upgrading. *Chem. Eng. J.* 313, 424–434.
- Gonçalves, A.L., Pires, J.C.M., Simões, M., 2017. A review on the use of microalgal consortia for wastewater treatment. *Algal Research* 24, 403–415.
- González-Fernández, C., Molinuevo-Salces, B., Cruz García-González, M., 2011. Nitrogen transformations under different conditions in open ponds by means of microalgae–bacteria consortium treating pig slurry. *Bioresour. Technol.* 102, 960–966.
- Henze, M., Gujer, W., Mino, T., Matsuo, T., van Loosdrecht, M.C.M., 2000. *Activated Sludge Models ASM1, ASM2, ASM2d and ASM3*. IWA Publishing, London.
- Henze, M., van Loosdrecht, M.C.M., Ekama, G.A., Brdjanovic, D., 2008. *Biological Wastewater Treatment: Principles, Modeling, and Design*. IWA Publishing, London.
- Jaramillo, F., Orchard, M., Muñoz, C., Zamorano, M., Antileo, C., 2018. Advanced strategies to improve nitrification process in sequencing batch reactors – a review. *J. Environ. Manag.* 218, 154–164.
- Judd, S., van den Broeke, L.J.P., Shurair, M., Kuti, Y., Znad, H., 2015. Algal remediation of CO<sub>2</sub> and nutrient discharges: a review. *Water Res.* 87, 356–366.
- Karya, N.G.A.L., van der Steen, N.P., Lens, P.N.L., 2013. Photo-oxygenation to support nitrification in an algal–bacterial consortium treating artificial wastewater. *Bioresour. Technol.* 134, 244–250.
- Kennish, M.J., de Jonge, V.N., 2011. Chemical introductions to the systems: diffuse and nonpoint source pollution from chemicals (nutrients: eutrophication). In: Kennish, M.J., Elliott, M. (Eds.), *Treatise on Estuarine and Coastal Science, Human-Induced Problems (Uses and Abuses)*, 8. Elsevier, Oxford.
- Krustok, I., Odlare, M., Shabimam, M.A., Truu, J., Truu, M., Ligti, T., Nehrenheim, E., 2015. Characterization of algal and microbial community growth in a wastewater treating batch photo-bioreactor inoculated with lake water. *Algal Research* 11, 421–427.
- Krustok, I., Odlare, M., Truu, J., Nehrenheim, E., 2016. Inhibition of nitrification in municipal wastewater-treating photobioreactors: effect on algal growth and nutrient uptake. *Bioresour. Technol.* 202, 238–243.
- Lee, C.S., Lee, S., Ko, S., Oh, H., Ahn, C., 2015. Effects of photoperiod on nutrient removal, biomass production, and algal–bacterial population dynamics in lab-scale photobioreactors treating municipal wastewater. *Water Res.* 68, 680–691.
- Leong, W., Lim, J., Lam, M., Yoshimitsu, U., Ho, C., Ho, Y., 2018. Co-cultivation of activated sludge and microalgae for the simultaneous enhancements of nitrogen-rich wastewater bioremediation and lipid production. *J. Taiwan Inst. Chem. Eng.* 87, 216–224.
- Li, Y., Chen, Y., Chen, P., Min, M., Zhou, W., Martinez, B., Zhu, J., Ruan, R., 2011. Characterization of a microalga Chlorella sp. well adapted to highly concentrated municipal wastewater for nutrient removal and biodiesel production. *Bioresour. Technol.* 102, 5138–5144.
- Liu, J., Wua, Y., Wu, C., Muylaert, K., Vyverman, W., Yu, H.Q., Muñoz, R., Rittmann, B., 2017. Advanced nutrient removal from surface water by a consortium of attached microalgae and bacteria: a review. *Bioresour. Technol.* 241, 1127–1137.
- Luo, Y., Le-Clech, P., Henderson, R.K., 2017. Simultaneous microalgae cultivation and wastewater treatment in submerged membrane photobioreactors: a review. *Algal Research* 24, 425–437.
- Luo, L., Dzakpasu, M., Yang, B., Zhang, W., Yang, Y., Wang, X.C., 2019. A novel index of total oxygen demand for the comprehensive evaluation of energy consumption for urban wastewater treatment. *Appl. Energy* 236, 253–261.
- Muñoz, R., Guieysse, B., 2006. Algal–bacterial processes for the treatment of hazardous contaminants: a review. *Water Res.* 40, 2799–2815.
- Rada-Ariza, A.M., Lopez-Vazquez, C.M., van der Steen, N.P., Lens, P.N.L., 2017. Nitrification by microalgal–bacterial consortia for ammonium removal in flat panel sequencing batch photo-bioreactors. *Bioresour. Technol.* 245, 81–89.
- Riño, B., Hernández, D., García-González, M.C., 2012. Microalgal-based systems for wastewater treatment: effect of applied organic and nutrient loading rate on biomass composition. *Ecol. Eng.* 49, 112–117.
- Subashchandrabose, S.R., Ramakrishnan, B., Megharaj, M., Venkateswarlu, K., Naidu, R., 2011. Consortia of cyanobacteria/microalgae and bacteria: biotechnological potential. *Biotechnol. Adv.* 29, 896–907.
- Sun, L., Zuo, W., Tian, Y., Zhang, J., Liu, J., Sun, N., Li, J., 2019. Performance and microbial community analysis of an algal-activated sludge symbiotic system: effect of activated sludge concentration. *J. Environ. Sci.* 76, 121–132.
- Tchobanoglous, G., Burton, F.L., Stensel, H.D., 2003. *Wastewater Engineering: Treatment and Reuse*, fourth ed. McGraw-Hill Metcalf & Eddy Inc., Boston.
- Tiron, O., Bumbac, C., Patroescu, I.V., Badescu, V.R., Postolache, C., 2015. Granular activated algae for wastewater treatment. *Water Sci. Technol.* 71, 832–839.
- Udayappan, A.F.M., Hassan, H.A., Takriff, M.S., Abdullah, S.R.S., 2017. A review of the potentials, challenges and current status of microalgae biomass applications in industrial wastewater treatment. *J. Water Process Eng.* 20, 8–21.
- Vargas, G., Donoso-Bravo, A., Vergara, C., Ruiz-Filippi, G., 2016. Assessment of microalgae and nitrifiers activity in a consortium in a continuous operation and the effect of oxygen depletion. *Electron. J. Biotechnol.* 23, 63–68.
- Vergara, C., Muñoz, R., Campos, J.L., Seeger, M., Jeison, D., 2016. Influence of light intensity on bacterial nitrifying activity in algal bacterial photobioreactors and its implications for microalgae-based wastewater treatment. *Int. Biodeterior. Biodegrad.* 114, 116–121.
- Vu, L., Loh, K., 2016. Symbiotic hollow fiber membrane photobioreactor for microalgal growth and bacterial wastewater treatment. *Bioresour. Technol.* 219, 261–269.
- Wagner, D., Valverde-Perez, B., Sæbø, M., de la Sotilla, M., Van Wagenen, J., Smets, B.F., Plosz, B., 2016. Towards a consensus-based biokinetic model for green microalgae – the ASM-A. *Water Res.* 103, 485–499.
- Wang, Y., Ho, S.H., Cheng, C.L., Guo, W.Q., Nagarajan, D., Ren, N.Q., Lee, D.J., Chang, J.S., 2016. Perspectives on the feasibility of using microalgae for industrial wastewater treatment. *Bioresour. Technol.* 222, 485–497.
- Wang, M., Keeley, R., Zalivina, N., Halfhide, T., Scott, K., Zhang, Q., van der Steen, P., Ergas, S.J., 2018. Advances in algal-prokaryotic wastewater treatment: a review of nitrogen transformations, reactor configurations and molecular tools. *J. Environ. Manag.* 217, 845–857.
- Ye, J., Liang, J., Wang, L., Markou, G., 2018. The mechanism of enhanced wastewater nitrogen removal by photo-sequencing batch reactors based on comprehensive analysis of system dynamics within a cycle. *Bioresour. Technol.* 260, 256–263.